Mon. Not. R. Astron. Soc. **277,** 1033–1046 (1995)

The timing noise of 45 southern pulsars

F. D'Alessandro,[1,2] P. M. McCulloch,[1] P. A. Hamilton[1] and A. A. Deshpande[1,3]

[1] *Physics Department, University of Tasmania, GPO Box 252C, Hobart, Tasmania, Australia 7001*
[2] *Department of Physical Sciences, University of Tasmania at Launceston, PO Box 1214, Launceston, Tasmania, Australia 7250*
[3] *Raman Research Institute, Bangalore 560 080, India*

Accepted 1995 June 30. Received 1995 June 26; in original form 1994 May 4

ABSTRACT

Pulse arrival-time data spanning up to 7 yr are analysed in order to provide a description of the timing noise of 45 southern pulsars. The results show that (i) for 19 pulsars, the timing activity is very weak (rms noise typically ≤ 2 milliperiods), (ii) for seven pulsars, the timing activity can be attributed to a random walk process comprising a large number of unresolvable events in one of the rotation variables, (iii) for seven pulsars, the timing activity can be attributed to resolved jumps in the rotation frequency and frequency derivative, superimposed on a random walk process, (iv) for seven pulsars, the timing activity can be attributed to resolved jumps, together with other low-level activity, and (v) for five pulsars, the timing activity is not due to a pure random walk process or resolved jumps. These results are discussed in the light of recent theories of mechanisms that may be responsible for pulsar timing noise.

Key words: methods: data analysis – stars: neutron – pulsars: general.

1 INTRODUCTION

After allowing for the deterministic pulsar spin-down ('pulsar braking') and any resolved period discontinuities ('glitches'), pulse arrival-time measurements display irregularities in the rotation rate of pulsars, commonly known as 'timing noise'. These irregularities exceed the uncertainties attributable to the measurement process. It has been proposed that this timing activity is the response of the neutron star to a 'noisy' component of the torque. This could arise from variations involving the moment of inertia or the magnetosphere of the neutron star.

Boynton et al. (1972) first suggested that rotational irregularities might arise from a simple 'random walk' process comprising unresolvable step functions in one of three observables – the pulse phase, ϕ ('phase noise', PN), frequency, ν ('frequency noise', FN) or frequency derivative, $\dot{\nu}$ ('slowing down noise', SN). The Crab pulsar timing noise was found to be consistent with a random walk in the pulse frequency (Boynton et al. 1972; Groth 1975). A similar analysis by Cordes & Helfand (1980) showed that the timing noise of a number of other pulsars could be described by a random walk process.

Detailed time-domain analyses of the timing behaviour in a sample of 24 pulsars by Cordes & Downs (1985) show that most timing activity cannot be modelled in terms of idealized, large-rate random walk processes. Instead, the activity appears to be due to discrete, identifiable events (microjumps) in one or more of the timing parameters (ϕ, ν or $\dot{\nu}$), possibly superimposed on an idealized random walk process, or a mixture of such processes.

Deeter & Boynton (1982) and Deeter (1984) have presented and discussed a frequency-domain approach to the description of timing noise in terms of the power spectrum of fluctuations in the rotation phase or one of its derivatives. Using this approach, Boynton & Deeter (1986) obtained noise power spectra for the same sample of pulsars as that studied by Cordes & Downs (1985). Alpar, Nandkumar & Pines (1986) have used the results to test theoretical models of timing noise. They conclude that the mechanism responsible for large-scale glitches plays no observable role in the timing noise of most pulsars.

The data analysed and presented in this paper were collected as part of a monthly timing survey of southern pulsars at the Mt Pleasant Observatory, operated by the Physics Department of the University of Tasmania. Details of the observations, data acquisition and reduction have been described elsewhere (D'Alessandro et al. 1993). The data are collected at two observing frequencies, 650 and 800 MHz, and at the time of writing, span a time interval of up to 7 yr. A preliminary analysis of the irregularities evident in the first 4 yr of timing data confirmed earlier results, namely that there is a significant correlation between timing activity and the rotation period derivative of pulsars. The timing noise of

a selection of pulsars from the Mt Pleasant sample is shown in Figs 1(a)–(d). The plots display the residual phase (after a second-order polynomial fit) as a function of time.

In this paper, we have used three different methods of analysis – estimation of strength parameters and structure functions, and statistical tests of microjumps in ν and $\dot{\nu}$. These tests are used to categorize the activity of each object, for example (i) a random walk process involving a large number of unresolvable events, (ii) a small number of resolved events, or (iii) a combination of both (i) and (ii).

2 DEFINITIONS AND TERMINOLOGY

2.1 Random walk processes

A random walk in the kth derivative of the phase is defined as (Groth 1975)

$$\frac{\mathrm{d}^k\phi(t)}{\mathrm{d}t^k}=\sum_j a_j H(t-t_j), \tag{1}$$

where a_j is a random amplitude with zero mean, H is a unit step function, and steps occur at times t_j. The random walks for $k=0, 1, 2$ correspond to PN, FN, SN respectively.

By definition, a random walk in the kth derivative of the phase is equivalent to a process where the $(k+1)$th derivative of the phase has stationary statistics, i.e. a white noise power spectrum (Groth 1975). Hence the phases arising from a random walk in the time derivatives of the pulse phase have non-stationary properties.

A number of authors (Groth 1975; Cordes 1980; Cordes & Greenstein 1981; Cordes & Downs 1985) have discussed the effect of the choice of the time origin used to describe the random walk. This is important if one is attempting to show that the time series of pulse arrival phases is consistent with a particular noise process. They conclude that it is satisfactory to take an arbitrary time, t_0, as the effective time origin as long as a second-order (or higher) polynomial is fitted to the phases (for $k\leq 2$). Such polynomial fitting is always done as part of the standard analysis procedure.

2.2 Strength parameters

The random walk processes described above can be studied by analysis of their second moment. To see whether such processes are responsible for the observed timing fluctuations, the estimated variance of the pulsar timing noise is compared with the variance expected for a random walk. The timing noise variance is estimated from

$$\sigma_{\mathrm{TN}}^2=\sigma_{\mathrm{R}}^2-\sigma_{\mathrm{W}}^2, \tag{2}$$

where $\sigma_{\mathrm{R}}^2=\sigma_{\mathrm{R}}^2(m, T)$ is the mean-square residual from an mth-order polynomial fit over a data span T, and

$$\sigma_{\mathrm{W}}^2=\sigma_{\mathrm{M}}^2+\sigma_{\mathrm{J}}^2 \tag{3}$$

is the mean-square white noise contribution from additive noise and pulse jitter (see Cordes & Downs 1985).

The random walks have second moments characterized by the *strength parameters*, S_k, where

$$S_0=R\langle(\Delta\phi)^2\rangle, \qquad S_1=R\langle(\Delta\nu)^2\rangle, \qquad S_2=R\langle(\Delta\dot{\nu})^2\rangle \tag{4}$$

(Cordes & Greenstein 1981). The $\langle\,\rangle$ denote an ensemble average, and $\Delta\phi$, $\Delta\nu$ and $\Delta\dot{\nu}$ are the unresolved steps in the rotation variables which occur with an average rate R. The strength parameters can be estimated from the rms residual, $\sigma_{\mathrm{TN}}(m, T)$, after performing a least-squares polynomial fit of order m over a data span T. Following Cordes (1980),

$$S_k=C_{k,m}^2\left[\frac{\sigma_{\mathrm{TN}}^2(m, T)}{\langle\sigma_{\mathrm{RW}}^2(T)\rangle_{\mathrm{u}}}\right]S_{\mathrm{u}}, \tag{5}$$

where $C_{k,m}$ are correction factors that compensate for the timing noise variance absorbed by the polynomial fit, and $\langle\sigma_{\mathrm{RW}}^2(T)\rangle_{\mathrm{u}}$ is the ensemble average second moment for a random walk of unit strength ($S_{\mathrm{u}}=1$). In practice, ensemble average quantities are not available. Instead, integral estimates of the moments such as

$$\langle\sigma_{\mathrm{RW}}^2(T)\rangle_{\mathrm{u}}=\frac{1}{T}\int_0^T \mathrm{d}t\,\phi_{\mathrm{RW}}^2(t) \tag{6}$$

can be made (Cordes & Greenstein 1981) or, for unevenly sampled data,

$$\langle\sigma_{\mathrm{RW}}^2(T)\rangle_{\mathrm{u}}=\frac{1}{N}\sum_{j=1}^{N}\langle\phi_{\mathrm{RW}}^2(t_j)\rangle, \qquad 0\leq t_1\leq t_N\leq T, \tag{7}$$

where $\langle\phi_{\mathrm{RW}}^2(t_j)\rangle$ is given by

$$S_0 t_j, \qquad \frac{1}{3}S_1 t_j^3, \qquad \frac{1}{20}S_2 t_j^5, \tag{8}$$

for PN, FN, SN respectively (Groth 1975; Cordes 1980) and assuming that the random walks are zero mean processes with unit strengths given by equation (4) with units of s^{-1}, $\mathrm{Hz}^2\,\mathrm{s}^{-1}$, $\mathrm{Hz}^2\,\mathrm{s}^{-3}$ respectively.

Consistency of one of the noise processes with the pulsar data is indicated if S_k is found to be independent of T and if the constraint $RT>1$ is satisfied (Cordes & Downs 1985). This consistency can be measured by using the statistic

$$F=\frac{S(T_{\max})}{S(T_{\min})}, \tag{9}$$

where $T_{\max}$ and $T_{\min}$ are the maximum and minimum time spans from which the strength parameter estimates can be obtained. If the data are consistent with a pure random walk process, then $F\approx 1$; otherwise F will be a strong function of $T_{\max}/T_{\min}$.

Following Cordes & Downs (1985), if $S(T_{\max})$ and $S(T_{\min})$ are statistically independent (derived from non-overlapping data spans) and have a Gaussian distribution, then $\log F$ will also have a Gaussian distribution with a standard deviation

$$\sigma_{\log F}=\sigma_{\log S}\left(1+\frac{1}{N_{\min}}\right)^{1/2}, \tag{10}$$

where $N_{\min}$ is the number of independent strength estimates used to estimate $S(T_{\min})$. It can be argued that $S(T_{\max})$ and $S(T_{\min})$ are essentially independent if $T_{\min}\ll T_{\max}$, since the random walk structure probed by each estimate is very different.

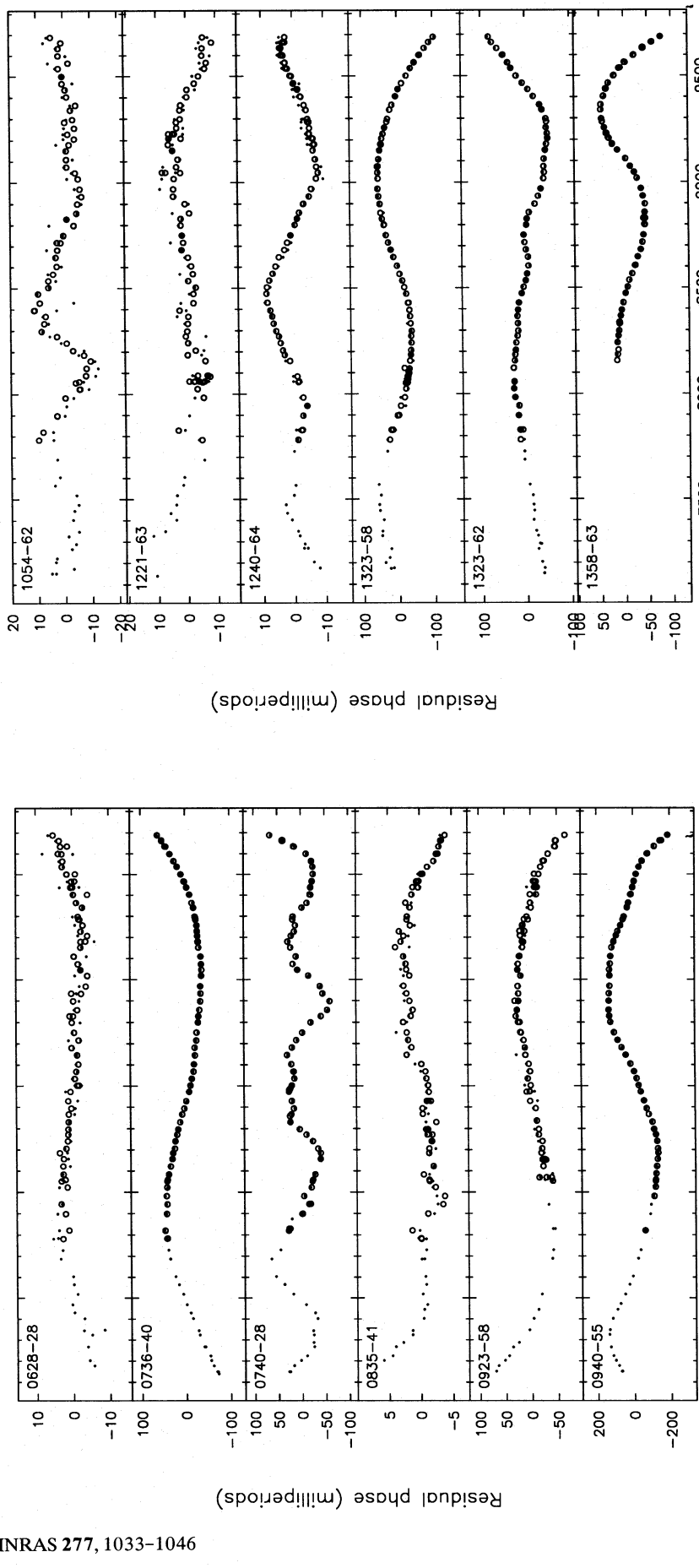

Figure 1. (a) Plots of phase residuals as a function of epoch, obtained from a second-order, least-squares polynomial fit for PSR 0628 − 28, 0736 − 40, 0740 − 28, 0835 − 41, 0923 − 58 and 9040 − 55, for both observing frequencies. (b) Plots as in (a) for PSR 1054 − 62, 1221 − 63, 1240 − 64, 1323 − 58, 1323 − 62 and 1358 − 63. (c) Plots as in (a) for PSR 1426 − 66, 1449 − 64, 1556 − 44, 1600 − 49, 1641 − 45 and 1648 − 42. (d) Plots as in (a) for PSR 1706 − 16, 1727 − 47, 1737 − 30, 1737 − 39, 1742 − 30 and 1749 − 28. Key: ● = 650-MHz data, ○ = 800-MHz data.

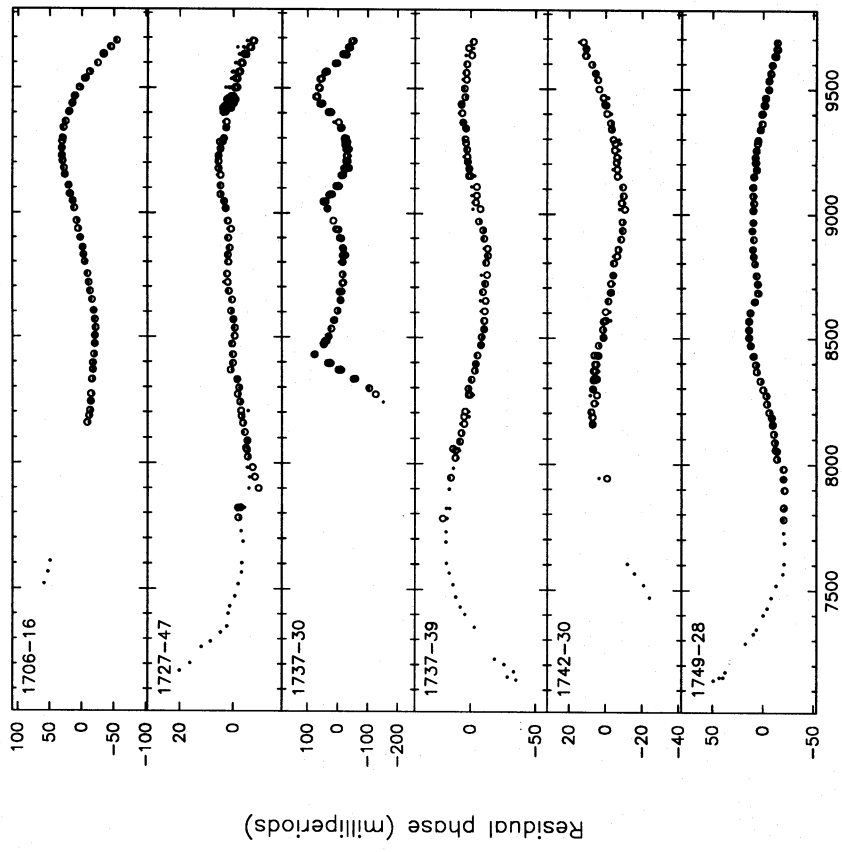

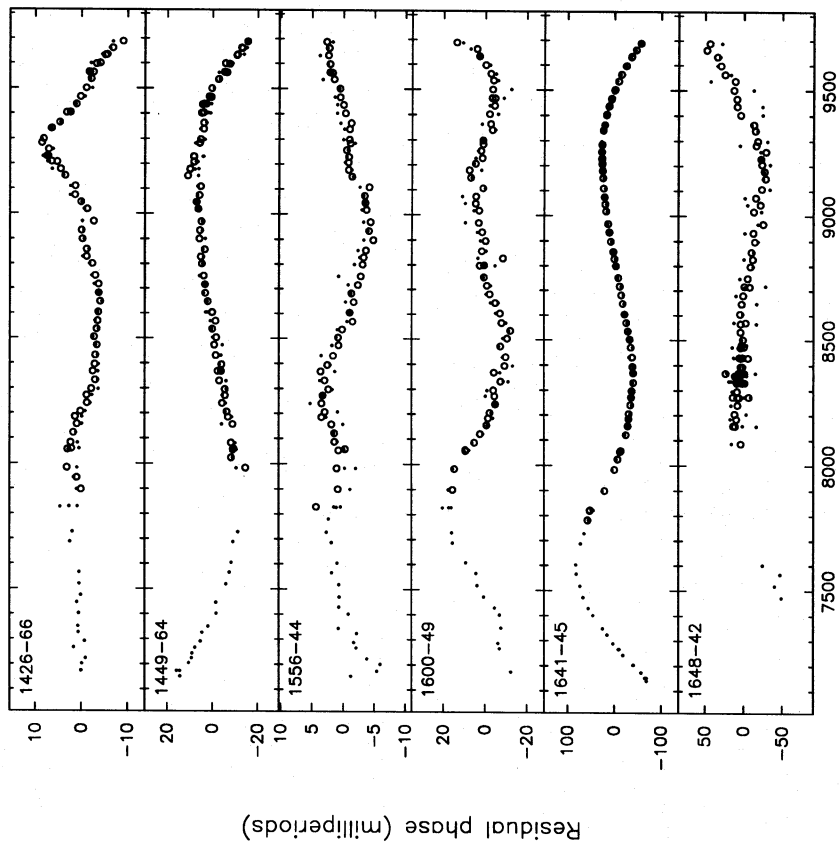

Figure 1 - *continued*

2.3 Structure functions

Structure functions are used to estimate the variance in a time series by means of a 'differencing scheme'. They provide a useful approach for the analysis of pulsar timing residuals where one is interested in examining the range of time-scales that contribute to the fluctuations. It is also possible to determine whether the fluctuations are significantly different from the activity due to a random walk process.

The mth-order structure function of the phase is defined as

$$D_{\phi}^{(m)}(t,\tau) \equiv \langle [\Delta_{\phi}^{(m)}(t,\tau)]^2 \rangle, \tag{11}$$

where

$$\Delta_{\phi}^{(m)}(t,\tau) \equiv \sum_{i=0}^{m} (-1)^i \binom{m}{i} \phi[t+(m-i)\tau] \tag{12}$$

is termed the mth increment of the phase (following Lindsay & Chie 1976 and Rutman 1978), τ is the time-scale probed by the differencing scheme, and t is the epoch of an individual phase measurement. The relevant features of these functions have been given by Cordes & Downs (1985). An idealized, large-rate, random walk process of order k has stationary $(k+1)$th increments, and hence the $(k+1)$th-order structure function is independent of time and has a unique power-law relationship with τ. For PN, $D_{\phi}^{(1)} \propto \tau$, giving a logarithmic slope (henceforth termed the 'structure function slope') of 1. Similarly, for FN, $D_{\phi}^{(2)} \propto \tau^3$, and for SN, $D_{\phi}^{(3)} \propto \tau^5$, giving slopes of 3 and 5 respectively.

3 ANALYSES AND RESULTS

Before any analyses were performed, we combined the dual-frequency phase residual data for each pulsar into a single data set. In addition to simplifying the interpretation of results, this procedure has two major advantages: (i) it improves the sensitivity of the data to be analysed, and (ii) it eliminates small dispersion measure variations which can produce phase fluctuations. Other frequency-dependent factors, such as refractive delays, are generally negligible at these observing frequencies, and their magnitude is very small in comparison to the measurement uncertainties in the data.

Table 1 shows some basic parameters for each of the 45 pulsars in our sample. The timing activity for 19 of these pulsars is too weak to allow a meaningful analysis (these are noted in the table). For these pulsars, the rms timing noise is typically ≤ 2 milliperiods and the signal-to-noise ratio ($S/N = \sigma_R/\sigma_W$) is typically ≤ 10, producing results from strength parameter and structure function analyses in the 'noise regime'. In the following sections, we present the results for the remaining 26 pulsars.

For five of the pulsars in Table 1, the standard arrival time analysis identified a number of discrete period jumps, both small ($\Delta\nu/\nu < 10^{-7}$) and large ($\Delta\nu/\nu \geq 10^{-7}$). PSR 1727−47 and 1737−30 have undergone one large jump each. The analysis and results of these timing observations will be published elsewhere. The data presented and analysed in this paper do not include these glitches. Allowance was made for these glitches in the arrival time analysis which produces the phase residuals. Small jumps were also noted for PSR 0740−28, 1240−64, 1641−45 and 1737−30 while fitting the data to standard timing models. The phase residuals for these pulsars include these jumps (see Fig. 1). However, subsequent analyses have been performed on the

Table 1. Basic observational parameters and noise estimates for 45 pulsars. The columns show the pulsar name and rotation period, and then the number of data points (N), data span (T_{max}), measurement uncertainty (σ_M), rms white noise (σ_W), rms timing noise (σ_{TN}) and the 'signal-to-noise ratio' of the timing noise, defined as the ratio σ_R/σ_W.

Pulsar PSR B	Period (s)	N	T_{max} (days)	σ_M (mP)	σ_W (mP)	σ_{TN} (mP)	S/N
0403-76[a]	0.5452	210	2461	0.71	1.99	1.86	7
0538-75[a]	1.2458	92	2536	0.50	0.94	0.94	7
0628-28	1.2444	83	2511	0.41	0.82	2.24	15
0736-40	0.3749	92	2549	0.38	0.48	30.96	321
0740-28	0.1667	112	2538	0.21	0.59	6.76	57
0740-28[b]	0.1667	112	2538	0.21	0.59	24.89	210
0808-47[a]	0.5471	76	2512	1.02	2.05	1.35	6
0835-41	0.7516	84	2486	0.12	0.25	1.96	40
0839-53[a]	0.7206	87	2458	0.93	2.62	1.74	6
0905-51[a]	0.2535	88	2511	0.97	2.53	3.31	8
0923-58	0.7395	92	2537	1.27	2.31	23.77	52
0932-52[a]	1.4447	83	2510	0.67	0.92	0.60	6
0940-55	0.6643	85	2537	0.56	1.19	95.04	400
0959-54	1.4365	88	2536	0.21	0.37	56.35	755
1054-62	0.4224	80	2537	0.80	0.97	4.78	25
1056-57[a]	1.1849	77	2489	0.67	1.04	1.11	7
1154-62[a]	0.4005	82	2537	0.96	1.15	2.42	12
1221-63	0.2164	80	2549	0.69	1.29	3.85	16
1240-64	0.3884	98	2513	0.14	0.20	0.37	11
1240-64[b]	0.3884	98	2513	0.14	0.20	4.48	115
1323-58	0.4779	105	2515	0.84	1.74	35.97	104
1323-62	0.5299	77	2537	0.56	1.26	31.59	126
1358-63	0.8427	81	1531	0.40	0.67	31.56	235
1426-66	0.7854	79	2516	0.17	0.40	3.61	45
1449-64	0.1794	83	2537	0.27	0.56	6.81	61
1451-68[a]	0.2633	88	2549	0.22	0.87	1.49	10
1530-53[a]	1.3688	82	2537	0.27	0.53	0.49	7
1556-44	0.2570	76	2536	0.21	0.31	2.25	36
1558-50	0.8642	85	2549	0.50	0.71	133.64	943
1600-49	0.3274	72	2516	0.74	1.43	6.73	24
1641-45	0.4550	91	2549	0.28	0.44	30.45	345
1641-45[b]	0.4550	91	2549	0.28	0.44	29.19	331
1648-42	0.8440	95	2217	1.42	3.75	13.63	19
1700-32[a]	1.2117	100	2524	0.59	0.92	0.69	6
1706-16	0.6530	60	2170	0.23	0.49	22.69	233
1718-32[a]	0.4771	84	2218	0.74	1.10	1.70	9
1727-47	0.8297	146	2515	0.18	0.30	3.38	57
1737-30	0.6066	154	1448	0.99	2.29	136.57	298
1737-30[b]	0.6066	154	1448	0.99	2.29	37.29	82
1737-39	0.5122	76	2548	0.69	0.86	9.54	56
1742-30	0.3674	68	2217	0.37	0.52	6.98	67
1747-46[a]	0.7423	75	2510	0.28	0.65	0.81	8
1749-28	0.5625	83	2548	0.09	0.38	12.78	169
1857-26[a]	0.6122	76	2541	0.63	0.71	0.90	8
1937-26[a]	0.4028	96	2393	0.68	1.67	0.50	5
2045-16[a]	1.9615	78	2541	0.16	0.32	0.63	11
2048-72[a]	0.3413	146	2487	0.56	2.88	2.23	6
2321-61[a]	2.3474	150	2458	0.45	0.82	0.75	7
2327-20[a]	1.6436	82	2522	0.32	0.65	0.92	9

[a]Indicates a pulsar that presently exhibits timing activity which is too weak for a meaningful analysis.
[b]Results obtained when periods jumps are not removed from the arrival time data.

phase residuals obtained from timing model fits made both with and without allowance for these small jumps.

3.1 Strength parameters

3.1.1 Strength parameter analysis

Strength parameters and their ratios were estimated from the pulsar phase residuals for each of the three random walk processes, in the manner described in Section 2.2. The estimates were made from blocks of data over octave time spans, i.e., $T_n = T_{max} 2^{-n}$ ($n = 0, 1, 2, \ldots$) with $N_n = 2^n$ such blocks for each octave in T. In most cases, $T_{max} \simeq 2500$ d and $T_{min} = 200$–300 d. Because of the restriction imposed by T_{min}, the maximum value of n was 3, which corresponds to $N_{min} = 8$ data blocks. Second-order polynomial fits were used to obtain the rms timing noise for the strength parameter computations, complemented by third-order fits for those pulsars whose phase residuals displayed an intrinsic cubic term and were not consistent with any of the random walk processes.

As a check on the method of analysis for the real data, strength parameter tests were performed on 500 realizations of random walks of order $k = 0, 1, 2$. Fig. 2 shows histograms of $\log(S_{est}/S)$ for each type of random walk process, where S_{est} and S correspond to the estimated and 'true' strength parameters respectively. The histograms follow roughly Gaussian distributions with standard deviations $\sigma_{\log S_{est}} \approx 0.21$, 0.40 and 0.50 for $k = 0$, 1, 2 random walks respectively. These results were independent of the signal-to-noise ratio, sampling rates and sampling patterns.

3.1.2 Strength parameter results and discussion

The results of the strength parameter analysis for these pulsars are shown in Table 2. The first entry for each pulsar corresponds to estimates obtained from the maximum (T_{max}) and minimum (T_{min}) time spans in the data. The second entry corresponds to estimates obtained from independent time spans, $T_{max}/2$ from one half of the data set, and T_{min} from the other half. Hence both estimates can be considered statistically independent – the first because $T_{min} \ll T_{max}$, and the second because of the independent time spans used to obtain the estimates.

In Table 2, column (2) lists the number of blocks (N_{min}, each spanning $T_{max}/8$ d) used to estimate $S(T_{min})$. The standard deviation in $\log[S(T_{min})]$ given in column (3) was determined from the set of N_{min} strength parameter estimates. Columns (4), (6) and (8) list the strength parameter ratios, F, for phase, frequency and slowing down noise respectively. Columns (5), (7) and (9) give the probabilities of obtaining values of F less than the estimated values. These probabilities can be calculated in two ways: (i) assuming an F-distribution with 1 and N_{min} degrees of freedom, and (ii) using the error function with a standard deviation given by equation (10). The probabilities given in Table 2 were obtained from the latter method. A probability around 0.5 suggests that the random walk under investigation is consistent with the data.

We find that idealized random walk processes do not account for all of the observed timing activity. After second-order fits, the phase residuals from eight pulsars, namely PSR 0628 – 28, 0835 – 41, 1054 – 62, 1221 – 63, 1426 – 66, 1556 – 44, 1600 – 49 and 1727 – 47, are consistent with a random walk in ϕ (PN). PSR 1449 – 64 shows consistency with PN only after third-order fits. The results for five pulsars, namely PSR 0736 – 40, 0940 – 55, 1323 – 58, 1323 – 62 and 1358 – 63, are consistent with a random walk in ν (FN). PSR 1240 – 64 shows consistency with FN if previously identified discrete events are not removed from the data. After third-order fits, PSR 1706 – 16 also shows consistency with FN. None of the results show consistency with a random walk in $\dot{\nu}$ (SN).

The results for the remaining 10 pulsars are inconsistent with all three pure random walk processes. The observed activity for these objects may be due to a mixture of random

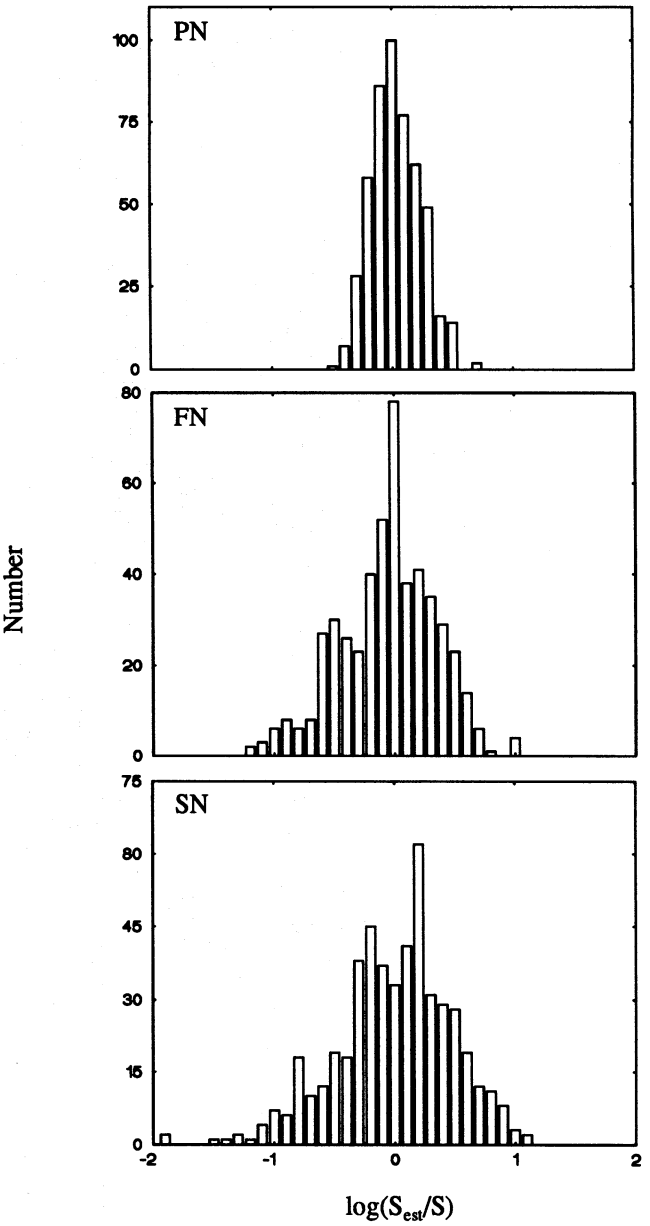

Figure 2. Histograms showing the distribution of strength parameter estimates obtained from 500 realizations of type $k = 0, 1, 2$ random walk processes (corresponding to PN, FN, SN). The simulations were generated using the same signal-to-noise ratio as the timing irregularities and sampling pattern as for PSR 0959 – 54.

Table 2. Results of the strength parameter analysis for 26 pulsars from second-order polynomial fits, supplemented by third-order fits in some cases. Consistency with one of the random walk processes is suggested by a ratio $F \approx 1$ over a range of time spans.

Pulsar PSR B	N_{min}	σ_{logS}	Strength parameter ratios and probabilities					
			F_{PN}	P_{PN}	F_{FN}	P_{FN}	F_{SN}	P_{SN}
(1)	(2)	(3)	(4)	(5)	(6)	(7)	(8)	(9)
0628-28	8	0.80	0.78	0.450	0.011	0.0099	0.0002	$< 10^{-4}$
	4		0.25	0.251	0.014	0.0193	0.0008	0.0003
0736-40	8	0.65	117.16	0.999	1.549	0.6085	0.0215	0.0078
	4		3.44	0.770	0.210	0.1753	0.0132	0.0048
0740-28	8	0.11	0.19	$< 10^{-3}$	0.003	$< 10^{-4}$	$< 10^{-4}$	$< 10^{-4}$
	4		0.30	$< 10^{-3}$	0.014	$< 10^{-4}$	0.0007	$< 10^{-4}$
0740-28[b]	8	0.16	2.27	0.980	0.030	$< 10^{-4}$	0.0004	$< 10^{-4}$
	4		4.36	1.000	0.267	0.0008	0.0181	$< 10^{-4}$
0835-41	8	0.39	2.70	0.852	0.040	0.0004	0.0006	$< 10^{-4}$
	4		1.13	0.550	0.063	0.0028	0.0037	$< 10^{-4}$
0923-58	7	0.55	4.32	0.859	0.069	0.0247	0.0011	$< 10^{-4}$
	3		0.10	0.061	0.008	0.0005	0.0005	$< 10^{-4}$
0923-58[a]	7	0.84	0.13	0.164	0.002	0.0016	$< 10^{-4}$	$< 10^{-4}$
	3		0.06	0.111	0.005	0.0090	0.0003	0.0002
0940-55	8	0.68	186.88	0.999	2.553	0.7128	0.0369	0.0241
	4		38.12	0.981	2.313	0.6832	0.1470	0.1380
0959-54	8	0.45	805.37	1.000	11.643	0.9866	0.1751	0.0581
	4		76.57	1.000	4.485	0.9004	0.2766	0.1358
0959-54[a]	8	0.57	165.70	1.000	2.406	0.7347	0.0371	0.0093
	4		10.01	0.941	0.636	0.3798	0.0422	0.0160
1054-62	8	0.98	1.10	0.516	0.016	0.0423	0.0003	0.0003
	4		0.11	0.191	0.006	0.0220	0.0004	0.0009
1221-63	8	0.54	1.35	0.591	0.023	0.0021	0.0003	$< 10^{-4}$
	4		0.79	0.431	0.051	0.0160	0.0035	$< 10^{-4}$
1240-64	7	0.50	0.25	0.132	0.003	$< 10^{-4}$	$< 10^{-4}$	$< 10^{-4}$
	4		1.55	0.634	0.084	0.0269	0.0047	$< 10^{-4}$
1240-64[b]	7	0.59	26.89	0.989	0.319	0.2142	0.0042	0.0001
	4		13.00	0.956	0.735	0.4192	0.0411	0.0171
1323-58	7	1.06	12.96	0.838	0.241	0.2921	0.0041	0.0173
	4		23.16	0.876	1.264	0.5344	0.0816	0.1783
1323-62	8	0.43	24.08	0.999	0.384	0.1795	0.0060	$< 10^{-4}$
	4		10.64	0.984	0.676	0.3610	0.0415	0.0019
1358-63	8	0.64	310.85	1.000	3.667	0.7953	0.0449	0.0244
	4		17.55	0.958	1.167	0.5370	0.0659	0.0507
1426-66	7	0.67	3.41	0.772	0.048	0.0325	0.0007	$< 10^{-4}$
	4		0.74	0.430	0.043	0.0339	0.0026	0.0003
1449-64	8	0.35	10.53	0.997	0.132	0.0090	0.0018	$< 10^{-4}$
	4		1.33	0.623	0.068	0.0014	0.0038	$< 10^{-4}$
1449-64[a]	6	0.73	0.44	0.324	0.005	0.0018	0.0001	$< 10^{-4}$
	4		1.19	0.536	0.062	0.0691	0.0035	0.0013
1556-44	8	0.81	1.18	0.534	0.018	0.0211	0.0003	$< 10^{-4}$
	4		0.14	0.174	0.009	0.0112	0.0006	0.0002
1558-50	8	0.43	388.77	1.000	5.189	0.9427	0.0747	0.0065
	4		2.24	0.768	0.122	0.0279	0.0072	$< 10^{-4}$
1600-49	8	0.28	2.79	0.934	0.040	$< 10^{-4}$	0.0006	$< 10^{-4}$
	4		2.23	0.868	0.125	0.0019	0.0074	$< 10^{-4}$
1641-45	8	1.17	47.45	0.912	0.646	0.4391	0.0092	0.0498
	4		3.60	0.665	0.205	0.2985	0.0122	0.0711
1641-45[b]	8	1.18	43.35	0.905	0.588	0.4267	0.0083	0.0481
	4		3.45	0.659	0.195	0.2953	0.0116	0.0711
1648-42	6	0.36	2.30	0.824	0.042	0.0002	0.0007	$< 10^{-4}$
	4		0.09	0.005	0.004	$< 10^{-4}$	0.0003	$< 10^{-4}$
1648-42[a]	6	0.30	0.18	0.012	0.003	$< 10^{-4}$	0.0001	$< 10^{-4}$
	4		0.07	$< 10^{-3}$	0.003	$< 10^{-4}$	0.0002	$< 10^{-4}$
1706-16	6	0.35	289.38	1.000	3.579	0.9294	0.0482	0.0002
	2		95.77	1.000	5.060	0.9505	0.2781	0.0964
1706-16[a]	6	0.35	61.04	1.000	0.757	0.3744	0.0102	$< 10^{-4}$
	2		5.47	0.957	0.294	0.1074	0.0164	$< 10^{-4}$
1727-47	8	0.78	2.56	0.688	0.026	0.0286	0.0003	$< 10^{-4}$
	4		0.29	0.268	0.013	0.0162	0.0007	0.0002
1737-30	8	0.42	481.35	1.000	5.562	0.9545	0.0715	0.0047
	4		13.68	0.993	0.767	0.4022	0.0410	0.0014
1737-30[a]	8	0.47	0.14	0.044	0.002	$< 10^{-4}$	$< 10^{-4}$	$< 10^{-4}$
	4		0.13	0.044	0.007	$< 10^{-4}$	0.0004	$< 10^{-4}$
1737-30[b]	8	0.47	14.15	0.990	0.183	0.0683	0.0026	$< 10^{-4}$
	4		60.37	1.000	3.386	0.8448	0.1810	0.0775
1737-39	8	0.74	6.26	0.846	0.098	0.0989	0.0016	0.0002
	4		9.38	0.881	0.552	0.3773	0.0353	0.0391
1742-30	6	0.39	15.59	0.998	0.244	0.0734	0.0038	$< 10^{-4}$
	4		0.39	0.174	0.018	$< 10^{-4}$	0.0010	$< 10^{-4}$
1749-28	8	0.77	15.21	0.926	0.211	0.2042	0.0030	0.0010
	4		4.10	0.762	0.241	0.2365	0.0152	0.0172

[a]Results obtained after third-order polynomial fits.
[b]Results obtained when periods jumps are not removed from the arrival time data.

walk processes (see Cordes & Greenstein 1981) or, alternatively, to 'microjumps' in the rotation frequency or frequency derivative. PSR 0740−28, 1240−64, 1641−45 and 1737−30 are likely examples of the latter possibility. For example, Flanagan (1993) has reported a small jump in ν and $\dot{\nu}$ for PSR 1641−45. This jump is also evident in our data, although the paucity of data around the time of the event precludes a detailed analysis. The jump accounts for a significant proportion of the observed timing noise.

In some cases, the phase residuals after third-order fits show little or no timing noise, i.e., they are essentially 'white'. However, the amplitude of the implied frequency second derivative ($\ddot{\nu}$) in each case was much too large to be attributed to pulsar braking.

3.2 Structure functions

3.2.1 Structure function analysis

Structure function estimates can be obtained from a span of data by using the definition given in Section 2.3, noting that the data represent the residual phase ($\delta\phi$) after a polynomial fit rather than the absolute phase (ϕ). For a random walk with $k=0$, 1, 2, the first-, second- and third-order structure functions of the residual phase [denoted by $D^{(1)}_{\delta\phi}(\tau)$, $D^{(2)}_{\delta\phi}(\tau)$ and $D^{(3)}_{\delta\phi}(\tau)$ respectively] will have theoretical logarithmic slopes of 1, 3 and 5 respectively.

Equation (11) represents an *ensemble average* structure function. In practice, we obtain structure function *estimates* from unevenly sampled data over a time span T by binning pairs of samples whose separations fall within a given range about some lag τ (Cordes & Downs 1985). Given the first-, second- and third-order phase increments as defined by equation (12), the structure function estimates are obtained from

$$D^{(1)}_{\delta\phi}(\tau)=N_\tau^{-1}\sum_{i,j}[\delta\phi(t_j)-\delta\phi(t_i)]^2, \tag{13}$$

$$D^{(2)}_{\delta\phi}(\tau)=N_\tau^{-1}\sum_{i,j,k}[\delta\phi(t_k)-2\delta\phi(t_j)+\delta\phi(t_i)]^2, \tag{14}$$

and

$$D^{(3)}_{\delta\phi}(\tau)=N_\tau^{-1}\sum_{i,j,k,l}[\delta\phi(t_l)-3\delta\phi(t_k)+3\delta\phi(t_j)-\delta\phi(t_i)]^2, \tag{15}$$

where N_τ is the number of terms in the sum.

To obtain reliable structure function estimates, it is important that the tolerance, ε, associated with the binning is chosen so that $1-\varepsilon \ll 1$. This is then used to bin pairs of samples logarithmically within a given range, namely,

$$\varepsilon\tau \le t_j - t_i \le \tau/\varepsilon. \tag{16}$$

Following Cordes & Downs (1985), we calculated the structure functions using $\varepsilon=0.89$, giving 10 bins per decade in τ. Fig. 3 is a typical logarithmic plot of the first-, second- and third-order structure functions as a function of the time lag, τ. The structure function slopes were obtained from linear least-squares fits to intermediate time lags of the logarithmic plots, bounded by the lags $\tau_{\min}$ and $\tau_{\max}$. The effects of additive noise and polynomial fits are responsible for restricting the slope estimates to these intermediate time lags (Cordes & Downs 1985).

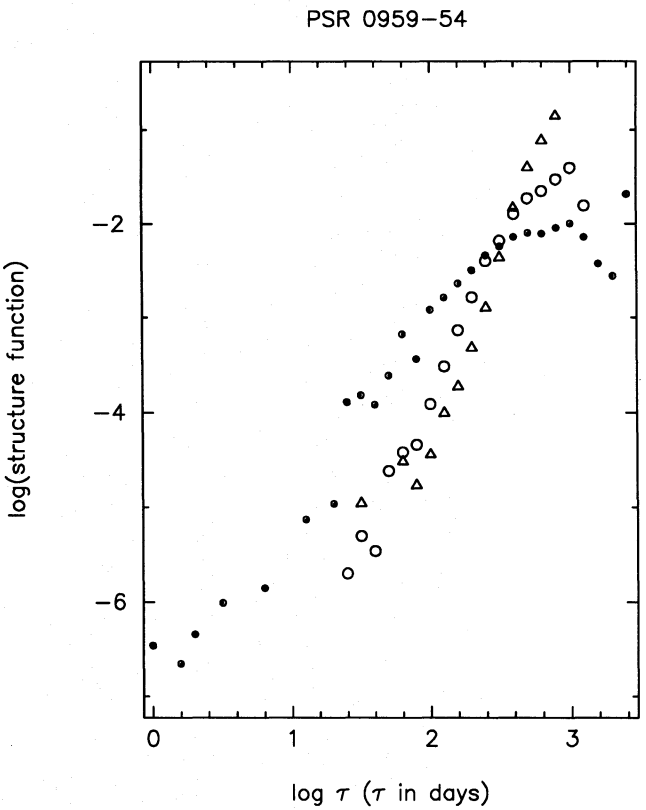

Figure 3. First-, second- and third-order structure functions of the timing noise in PSR 0959 − 54. Key: ● = $D^{(1)}_{\delta\phi}$, ○ = $D^{(2)}_{\delta\phi}$, △ = $D^{(3)}_{\delta\phi}$.

Table 3. Mean structure function slopes obtained from 20 random walk simulations using (a) uniform 30-d sampling (the approximate interval between observations), and (b) uneven sampling, corresponding to the observations of PSR 0959 − 54. The slopes obtained from the structure function estimates are close to the theoretical values, and show that the estimation method is relatively insensitive to the sampling pattern.

Random walk	$\tau_{\min}$ (days)	$\tau_{\max}$ (days)	Structure function slopes $D^{(1)}_{\delta\phi}$	Err	$D^{(2)}_{\delta\phi}$	Err	$D^{(3)}_{\delta\phi}$	Err
PN[a]	32,63,100	500	1.0	2	1.2	3	1.4	5
FN[a]	32,63,100	500	1.8	1	3.0	3	3.4	5
SN[a]	32,63,100	500	2.0	1	3.7	3	4.9	5
PN[b]	32,63,100	500	1.0	2	1.1	4	1.2	6
FN[b]	32,63,100	500	1.8	2	2.8	5	3.3	6
SN[b]	32,63,100	500	1.9	1	3.6	3	4.6	5

[a]The random walk time series was uniformly sampled at 30-d intervals.
[b]The random walk time series was sampled at the same epochs as the data from PSR 0959 − 54.

As a check on the method of analysis, we performed tests on simulated random walks, using both uniform sampling and uneven sampling corresponding to the observations of PSR 0959 − 54. Table 3 shows the mean results of these tests for 20 realizations of a random walk in ϕ, ν and $\dot{\nu}$. The

columns contain, respectively, the type of random walk process, the minimum (τ_{min}) and maximum (τ_{max}) time lags over which the first-, second- and third-order structure function slopes were computed, and the mean slope of each structure function and their 1σ uncertainties, which refer to the last digit quoted. The results show that the structure function slopes are close to the theoretical values, and that the estimates are insensitive to the sampling pattern of the data.

3.2.2 *Structure function results and discussion*

The results for the actual pulsar data are summarized in Table 4. The uncertainties in the structure function slopes are the 1σ formal errors and refer to the last digit quoted.

After second-order polynomial fits, we find that (i) for PSR 0628−28, 0835−41, 1054−62, 1221−63, 1426−66, 1556−44, 1600−49 and 1727−47, the phase residuals are consistent with PN, (ii) for PSR 0736−40, 0940−55, 1323−58, 1323−62, 1358−63, 1558−50, 1641−45 and 1706−16, the phase residuals are consistent with FN, (iii) none of the results show consistency with SN (with the possible exception of PSR 1641−45, using data which includes the discrete events), and (iv) for the remaining 10 pulsars, the phase residuals are not consistent with any of the pure random walk processes. In general, these results are consistent with the conclusions drawn from the strength parameter analysis.

The structure function slopes for some of the remaining pulsars are approximately square-law in $D^{(1)}_{\delta\phi}$, cubic or higher

Table 4. Results of the structure function analysis for 26 pulsars after second-order polynomial fits, supplemented in a few cases with the results after third-order fits.

Pulsar	τ_{min}	τ_{max}	Structure function slopes					
PSR B	(days)	(days)	$D^{(1)}_{\delta\phi}$	Err	$D^{(2)}_{\delta\phi}$	Err	$D^{(3)}_{\delta\phi}$	Err
0628-28	10,100,125	400,700,800	0.72	7	1.07	9	1.5	3
0736-40	6,60,60	320,630,630	1.88	9	3.14	6	3.0	2
0740-28	6,30,40	100,150,150	1.9	2	1.1	5	0.8	5
0740-28[b]	15,40,60	150,320,320	2.1	3	1.8	2	2.6	3
0835-41	16,30,30	500	1.1	1	1.40	9	1.2	2
0923-58	25,125,250	630,800,800	1.32	5	2.5	2	5.5	3
0923-58[a]	25,25,60	400,630,500	0.30	5	0.23	5	0.4	1
0940-55	10,30,60	630	1.70	9	3.0	2	3.3	3
0959-54	6,80,100	320	2.1	1	3.3	1	4.0	2
0959-54[a]	15,30,60	500	1.53	7	3.1	1	3.6	1
1054-62	30	320	1.11	8	1.3	2	1.5	5
1221-63	30,60,60	800	0.93	6	1.07	6	1.7	2
1240-64	15,25,30	1000	0.31	6	0.4	1	0.3	1
1240-64[b]	10,80,100	400,500,500	1.70	6	3.0	1	3.5	2
1323-58	10,100,100	500,500,630	1.80	5	3.3	1	3.5	5
1323-62	10,60,80	250,500,800	1.9	1	2.6	2	3.0	8
1358-63	25,25,30	400	1.47	8	3.22	9	3.7	6
1426-66	20,40,40	320,400,400	1.37	7	1.6	2	1.9	2
1449-64	10,40,60	400,800,800	1.48	7	1.98	3	2.2	3
1449-64[a]	10,30,80	400	0.6	2	0.6	3	0.4	4
1556-44	30,80,100	630	1.03	5	1.83	6	1.73	6
1558-50	3,30,30	320,320,800	2.3	2	3.6	5	3.3	3
1600-49	20,30,50	500	1.18	8	1.82	8	2.1	1
1641-45	25,40,50	500	1.70	7	2.97	8	3.5	2
1641-45[b]	15,50,100	400,400,500	1.67	7	3.5	2	4.6	3
1648-42	50,100,160	630	1.25	9	1.9	3	3.3	4
1648-42[a]	10,30,30	630	0.13	9	0.4	1	0.6	2
1706-16	25,50,100	150,250,630	1.7	2	3.3	2	3.9	4
1706-16[a]	15,60,100	320,320,500	1.7	1	3.3	1	3.7	2
1727-47	15,25,100	250,250,630	1.12	9	1.1	3	1.9	2
1737-30	25,25,100	500	1.52	4	3.2	1	5.63	8
1737-30[a]	10,10,30	500	0.17	4	0.28	7	0.6	1
1737-30[b]	10,15,50	160	2.2	2	2.4	2	5.2	6
1737-39	40,80,200	400,630,800	1.6	2	2.76	6	3.9	1
1742-30	25,160,320	630	1.54	4	3.3	2	6.8	5
1742-30[a]	15,40,60	500	0.65	6	0.71	8	0.9	2
1749-28	30,30,80	400,630,800	1.8	1	2.3	1	3.0	2

[a]Results obtained after third-order polynomial fits.
[b]Results obtained when periods jumps are not removed from the arrival time data.

in $D^{(2)}_{\delta\phi}$, and large in $D^{(3)}_{\delta\phi}$ (≥ 4), suggesting that the phase residuals may be dominated by one or more discrete events in $\dot{\nu}$. After removing a third-order polynomial, the phase residuals for PSR 0923−58, 1449−64, 1648−42, 1737−30 and 1742−30 are essentially 'white', giving structure function slopes <1.

The strength parameter and structure function analyses have demonstrated that the timing activity of a number of pulsars is not consistent with an idealized random walk process. Hence it is necessary to analyse the phase residuals for discrete events (microjumps) in ν and $\dot{\nu}$. These events may account for much of the observed timing activity of these pulsars.

3.3 Discrete events

The significance of discrete events in ν and $\dot{\nu}$ can be tested by comparing the amplitudes of $\Delta\nu$ and $\Delta\dot{\nu}$ with the standard deviation of a large-rate, random walk process. For events in ν and $\dot{\nu}$, the standard deviations are given by $\sigma_{\Delta\nu}=\sqrt{S_1\Delta t}$ and $\sigma_{\Delta\dot{\nu}}=\sqrt{S_2\Delta t}$ respectively (Cordes & Downs 1985). The tests are performed at a given 'significance level', N, where a discrete event is considered real if $\Delta\nu/\sigma_{\Delta\nu}\geq N$ or $\Delta\dot{\nu}/\sigma_{\Delta\dot{\nu}}\geq N$. This test for $\Delta\nu$ is essentially the same as that proposed by Cordes & Helfand (1980), except that the parameter they tested was the ratio of variances, $r=\Delta\nu^2/(N\sigma_{\Delta\nu})^2$, with $N=3$. The latter test was previously used to assess the significance of apparent period discontinuities observed in PSR 0740−28 and 1737−30 (D'Alessandro et al. 1993).

3.3.1 *Method of analysis of discrete events*

For each of the 26 pulsars suitable for analysis, we averaged phase residuals over 3–4 d, and then computed the numerical derivative. The resultant frequency residuals, $\delta\nu(t)$, were relatively free of large noise spikes which can arise from measurement uncertainties when the derivative is computed from closely spaced observations.

Plots of the phase residuals used for the analysis of 24 pulsars are shown in Figs 1(a)–(d). Fig. 4 shows the two remaining cases, where $\delta\nu(t)$ are also plotted. Phase residual plots for the other 19 pulsars which exhibit little timing activity can be found in D'Alessandro et al. (1993). Note that the sign of the phase residuals in these plots is defined in the sense of 'observed minus predicted *arrival time*'. This is consistent with the past use of downward-veering phase residuals to represent a discontinuous increase in the rotation frequency of the Vela pulsar (McCulloch et al. 1987, 1990). The numerical derivatives have been inverted to obtain frequency residuals of the correct sign.

Following Cordes & Downs (1985), we used the $\delta\nu(t)$ data to identify the epochs of discrete events and modelled them with a small number of piecewise linear segments. Estimates of $\Delta\nu$ and $\Delta\dot{\nu}$ were then obtained from least-squares fits to the data either side of the event. In order to allow for measurement uncertainties, events were considered real only if the magnitude of the observed jump was greater than 5σ (i.e. $N=5$). Experiments on simulated random walk data with similar signal-to-noise ratios as the real data demonstrated the reliability of this test, correctly rejecting fluctuations in the random walk process which appeared to be real.

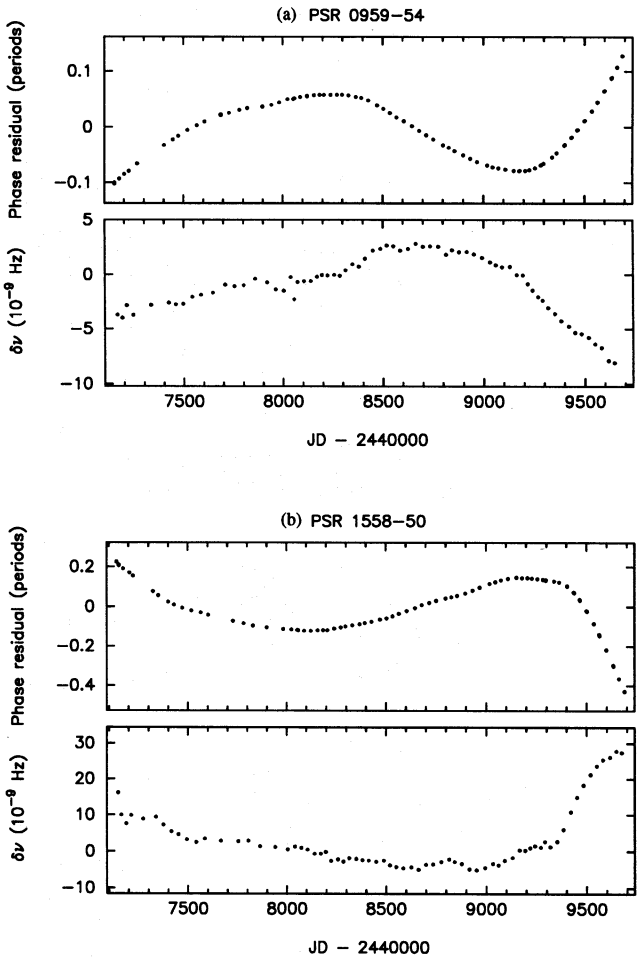

Figure 4. Phase residuals resulting from a second-order, least-squares polynomial fit and their first derivative, plotted as a function of epoch for (a) PSR 0959−54, and (b) PSR 1558−50.

An additional condition was imposed on the significance tests – the jump amplitude had to be significant with respect to the 'formal' error of the jump estimate, given approximately by $\delta(\Delta\nu)=\sqrt{2}\sigma_{\rm w}/\Delta t$ (where $\Delta t\simeq 30$ d) and $\delta(\Delta\dot{\nu})=\sqrt{\delta m_1^2+\delta m_2^2}$ (where δm_1 and δm_2 are the errors from the linear fits used to compute $\Delta\dot{\nu}$).

Two methods, A and B, were used to compute S_1 and S_2 and hence the standard deviation for FN and SN. Following Cordes & Downs (1985), for method A we used the data between two events where timing activity was less than usual, and for method B, we used the whole data set. The rms phase using method A tends to be dominated by events in ν, while for method B, it is dominated by events in $\dot{\nu}$. Hence greater weight was placed on method A for testing events in ν, and method B for testing events in $\dot{\nu}$.

3.3.2 *Results of tests for discrete events*

Table 5 shows the results of the significance tests on discrete events in ν and $\dot{\nu}$ for 26 pulsars. Columns (3)–(15) contain, respectively, the event epoch and its uncertainty Δt, the amplitude of the jumps in ν and $\dot{\nu}$, the logarithm of the strength parameters used to compute the standard deviation

Table 5. Results of statistical tests on discrete events in ν and $\dot{\nu}$. See the text for an explanation of each column.

Pulsar PSR B	Event	Epoch (TJD)	Δt (days)	$\Delta\nu$ (†)	$\Delta\dot{\nu}$ (§)	$\log S_1$ ($\mathrm{Hz^2 s^{-1}}$)		$\log S_2$ ($\mathrm{Hz^2 s^{-3}}$)		$\lvert\Delta\nu/\sigma_{\Delta\nu}\rvert$		$\lvert\Delta\dot{\nu}/\sigma_{\Delta\dot{\nu}}\rvert$		Real events
						A	B	A	B	A	B	A	B	
[1]	[2]	[3]	[4]	[5]	[6]	[7]	[8]	[9]	[10]	[11]	[12]	[13]	[14]	[15]
0628-28	1	7802	38	+0.3	+0.04	-26.3	-26.9	-39.7	-41.8	2.5	5.0	0.2	1.5	$\Delta\nu$
	2	9193	27	−0.1	−0.05					1.3	2.7	0.3	2.7	
0736-40	1	7645	83	+1.1	+0.3	-25.3	-24.7	-38.7	-39.5	1.9	0.8	0.2	0.5	
	2	8283	25	+0.1	−0.78					0.4	0.2	1.3	3.0	
	3	9319	42	−0.6	−0.48					1.6	0.7	0.6	1.4	
0740-28	1	7645	83	+11	+2.5	-23.5	-24.8	-36.1	-39.6	2.3	10.3	0.1	6.2	$\Delta\nu$,$\Delta\dot{\nu}$
	2	8344	28	+3	+0.1					0.9	4.0	0.0	0.6	
	3	8664	36	+4	+3.3					1.3	6.1	0.2	12.2	$\Delta\nu$,$\Delta\dot{\nu}$
	4	8878	41	−11	−0.7					3.2	14.5	0.0	2.4	$\Delta\nu$
	5	9319	42	−3	−6.7					0.8	3.7	0.4	23.3	$\Delta\dot{\nu}$
0835-41	1	7860	78	+0.2	+0.12	-26.5	-27.0	-40.1	-41.8	1.6	2.9	0.5	3.7	
0923-58	1	8001	116	−0.5	+0.9	-25.6	-24.9	-39.4	-39.8	0.9	0.4	1.6	2.2	
0940-55	1	7460	29	−0.7	−8.1	-24.0	-23.7	-36.8	-38.5	0.4	0.3	1.3	9.0	$\Delta\dot{\nu}$
	2	8171	29	−2	−1.7					1.0	0.7	0.3	1.9	
	3	8452	42	+1	+0.9					0.7	0.5	0.1	0.9	
	4	8699	35	−0.4	+6.5					0.2	0.2	0.9	6.5	$\Delta\dot{\nu}$
	5	8879	42	+0.7	−6					0.4	0.2	0.7	5.1	$\Delta\dot{\nu}$
	6	9032	28	−0.8	+4					0.5	0.4	0.7	5.0	$\Delta\dot{\nu}$
	7	9270	29	−1.5	−4.5					0.9	0.6	0.7	5.0	$\Delta\dot{\nu}$
	8	9483	35	+1.6	+9.3					0.9	0.6	1.4	9.4	$\Delta\dot{\nu}$
0959-54	1	7543	48	+0.2	+0.3	-26.2	-24.1	-39.2	-39.0	1.2	0.1	0.5	0.4	
	2	7920	46	−0.8	−0.3					5.0	0.4	0.5	0.4	$\Delta\nu$
	3	8313	33	+0.5	+0.8					3.6	0.3	1.9	1.4	
	4	8587	36	−0.1	−1.6					0.5	0.1	3.7	2.7	
	5	9130	41	−0.9	−1.84					6.3	0.6	3.9	3.0	$\Delta\nu$
	6	9451	29	+0.2	+0.3					1.5	0.1	0.7	0.5	
1054-62	1	8140	35	−1.9	−0.1	-26.4	-26.2	-40.7	-41.1	17.7	14.7	0.8	1.2	$\Delta\nu$
	2	8285	25	+1.6	−0.1					16.9	13.9	1.4	2.0	$\Delta\nu$
1221-63	1	9130	42	+0.1	+0.1	-26.9	-26.5	-41.5	-41.4	0.8	0.5	2.1	1.8	
1240-64	1	7454	41	+0.4	+0.01	-27.1	-26.3	-40.5	-41.1	7.4	3.0	0.1	0.1	$\Delta\nu$
	2	7963	40	−0.5	−0.03					9.6	3.9	0.3	0.5	$\Delta\nu$
	3	8488	31	+0.5	+0.01					10.0	4.1	0.1	0.2	$\Delta\nu$
	4	9032	28	−0.6	−0.06					12.8	5.2	0.8	1.5	$\Delta\nu$
1323-58	1	7648	160	+0.8	−1.5	-25.6	-24.5	-39.0	-39.3	1.3	0.4	1.2	1.8	
	2	8139	36	−1.3	+0.5					4.8	1.3	1.0	1.4	
	3	8626	42	−0.6	+1.7					2.0	0.6	2.7	4.0	
1323-62	1	8626	42	−2.5	+1.7	-25.2	-24.6	-38.3	-39.5	5.6	2.7	1.3	4.7	$\Delta\nu$
	2	8916	37	−1.6	−2.9					3.8	1.8	2.4	8.7	$\Delta\dot{\nu}$
	3	9352	24	−2.7	+1.2					7.9	3.8	1.2	4.4	$\Delta\nu$
1358-63	1	8551	31	+0.6	−1.8	-25.3	-23.9	-38.8	-38.3	1.6	0.3	2.8	1.5	
	2	9092	36	−1.8	+3.91					4.9	0.9	5.7	3.1	$\Delta\nu$,$\Delta\dot{\nu}$
1426-66	1	8020	74	+0.1	−0.07	-27.0	-26.5	-41.2	-41.3	1.4	0.8	1.2	1.4	
	2	9291	16	+0.8	+0.01					21.8	12.5	0.5	0.6	$\Delta\nu$
1449-64	1	7856	255	−0.4	+0.13	-26.9	-26.0	-41.0	-40.8	2.3	0.8	0.9	0.7	
	2	9131	43	+0.3	+0.20					4.0	1.4	3.4	2.7	
1556-44	1	8257	32	+0.2	+0.03	-26.4	-26.9	-40.0	-41.8	1.7	3.1	0.2	1.4	
	2	8878	42	−0.3	−0.01					2.5	4.5	0.0	0.2	
1558-50	1	7585	38	+0.7	+1.8	-25.1	-23.4	-37.4	-38.2	1.4	0.2	0.5	1.3	
	2	8224	34	−1.9	+0.42					3.7	0.5	0.1	0.3	
	3	8952	36	+0.1	+2.6					0.2	0.0	0.7	1.9	
	4	9319	41	+0.6	+11.1					1.0	0.2	2.8	7.7	$\Delta\dot{\nu}$
	5	9550	28	+2.1	−9.6					4.5	0.7	2.9	8.1	$\Delta\dot{\nu}$
1600-49	1	8105	34	−0.6	−0.26	-25.5	-26.0	-39.0	-40.8	1.8	3.1	0.5	4.0	
	2	9129	42	+0.5	−0.2					1.6	2.7	0.3	2.6	
1641-45	1	7645	85	+2.7	−1.3	-25.9	-24.7	-39.5	-39.5	9.0	2.1	2.6	2.8	$\Delta\nu$
	2	7860	78	+2.2	−1.1					7.9	1.9	2.5	2.6	$\Delta\nu$
	3	8487	32	+0.1	+0.90					0.6	0.1	3.0	3.2	
	4	8878	42	+0.1	+0.42					0.6	0.1	1.2	1.3	
	5	9291	13	+0.4	+0.79					3.8	0.9	4.1	4.4	
1648-42	1	8587	37	+0.6	−0.5	-25.3	-25.3	-39.4	-40.0	1.4	1.4	1.4	3.0	
1706-16	1	7883	49	−0.7	−0.1	-27.0	-24.8	-39.9	-39.5	3.5	0.3	0.2	0.1	
	2	8552	33	−0.7	+0.01					14.3	1.1	0.1	0.0	$\Delta\nu$
	3	9131	43	−0.4	+1.5					7.3	0.6	6.9	4.4	$\Delta\nu$,$\Delta\dot{\nu}$
	4	9420	34	+0.1	−0.1					2.4	0.2	0.7	0.5	
1727-47	1	7860	77	+0.4	+0.15	-26.3	-26.6	-39.7	-41.4	2.1	2.9	0.4	3.0	
	2	9192	28	+0.2	+0.13					2.2	3.0	0.6	4.4	

Table 5 – *continued*

Pulsar PSR B	Event	Epoch (TJD)	Δt (days)	$\Delta\nu$ (†)	$\Delta\dot{\nu}$ (§)	$\log S_1$ (Hz^2s^{-1}) A	$\log S_1$ (Hz^2s^{-1}) B	$\log S_2$ (Hz^2s^{-3}) A	$\log S_2$ (Hz^2s^{-3}) B	$\lvert\Delta\nu/\sigma_{\Delta\nu}\rvert$ A	$\lvert\Delta\nu/\sigma_{\Delta\nu}\rvert$ B	$\lvert\Delta\dot{\nu}/\sigma_{\Delta\dot{\nu}}\rvert$ A	$\lvert\Delta\dot{\nu}/\sigma_{\Delta\dot{\nu}}\rvert$ B	Real events
[1]	[2]	[3]	[4]	[5]	[6]	[7]	[8]	[9]	[10]	[11]	[12]	[13]	[14]	[15]
1737-30	1	8451	42	+23	+3.7	-25.2	-23.7	-36.1	-38.0	49.7	8.5	0.2	2.1	$\Delta\nu$
	2	9061	28	+14	−2.9					36.4	6.2	0.2	2.0	$\Delta\nu$
	3	9484	35	+12	−2					27.7	4.7	0.1	1.2	$\Delta\nu$
	4	9581	34	+6	+4.0					14.4	2.5	0.4	2.5	$\Delta\nu$
1737-39	1	7964	39	+0.3	−0.48	-26.4	-25.7	-40.1	-40.5	2.6	1.2	2.8	4.8	
	2	8994	50	−0.4	+0.35					2.7	1.2	1.8	3.1	
1742-30	1	8843	28	−0.3	−0.24	-26.7	-25.8	-40.5	-40.5	4.5	1.7	2.9	2.8	
1749-28	1	7646	83	−0.2	+0.34	-26.4	-25.4	-39.1	-40.2	1.3	0.4	0.5	1.6	
	2	8451	42	+0.2	+1.3					1.3	0.4	2.6	9.1	$\Delta\dot{\nu}$
	3	8700	36	−1.6	−1.0					14.6	4.6	2.1	7.5	$\Delta\nu$,$\Delta\dot{\nu}$

† In units of 10^{-9} Hz.
§ In units of 10^{-16} Hz s^{-1}.

for FN and SN (using both methods A and B), the significance level of the magnitude of $\Delta\nu$ and $\Delta\dot{\nu}$ for each event (using both methods A and B), and an indication of which events can be considered real.

A total of 76 events in ν and $\dot{\nu}$ were considered using the 5σ threshold test. For the $\Delta\nu$ events, six are significant using both methods, 15 are significant using method A only, four are significant using method B only, and 51 were not significant. For the $\Delta\dot{\nu}$ events, two are significant using method A only, 14 are significant using method B only, and the remaining 60 events were not significant using either method. Column (15) of Table 5 indicates which events we consider to be real, taking account of the results of both the strength parameter and structure function analyses. Of the 76 discrete events tested, 33 of the events in ν, and 34 of the events in $\dot{\nu}$ have a negative amplitude. Of the discrete events which passed the threshold test, 12 out of the 26 events in ν, and seven out of the 16 events in $\dot{\nu}$ have a negative amplitude.

3.4 Summary of results

In this section, we summarize the timing activity of individual pulsars, based on the results from the previous sections.

The data obtained from PSR 0403−76, 0538−75, 0808−47, 0839−53, 0905−51, 0932−52, 1056−57, 1154−62, 1451−68, 1530−53, 1700−32, 1718−32, 1747−46, 1857−26, 1937−26, 2045−16, 2048−72, 2321−61 and 2327−20 show little or no timing activity. The results of the analyses for PSR 0628−28, 0835−41, 1054−62, 1221−63, 1426−66, 1556−44, 1600−49 and 1727−47 are roughly consistent with a random walk in ϕ. Tests on discrete events indicate that jumps are significant, all in ν, for three of these pulsars (see Table 5).

PSR 0736−40. The analyses suggest the behaviour of this pulsar is consistent with a random walk in ν. No discrete events were found to be significant with respect to a 5σ threshold test.

PSR 0740−28. The results of the strength parameter and structure function analyses are not consistent with a pure random walk process. The 5σ threshold tests on the discrete events indicate that three $\Delta\nu$ and $\Delta\dot{\nu}$ events are significant. Smaller events are also evident in the phase residuals, occurring every 100–200 d. However, these could not be tested due to the paucity of data between each event.

PSR 0923−58. The results for this pulsar are not consistent with a pure random walk process, and there are no discrete events. Timing noise is dominated by a large cubic term. Little timing activity is evident after a third-order polynomial fit. However, the amplitude of the implied frequency second derivative is much too large to be attributed to pulsar braking. A single, unresolved jump in ν or $\dot{\nu}$ could easily give rise to such a cubic term. This interpretation is supported by the structure function analysis which gave a large slope (5.5) for $D^{(3)}_{\delta\phi}$.

PSR 0940−55. The results of the strength parameter and structure function analyses show reasonable consistency with a random walk in ν. Also, six events in $\dot{\nu}$ are significant. Three of these events have a negative amplitude.

PSR 0959−54. The results are not consistent with a pure random walk process. It appears that some of the activity is due to discrete events. Two events in ν were found to be significant.

PSR 1240−64. The phase residuals for this pulsar appear piecewise linear, indicating events in ν which occur roughly once every 500 d. All four such events appear to be significant. An interesting feature of these jumps is their alternating nature. Continued monitoring of this pulsar will enable a more detailed analysis of the observed trend. The strength parameter and structure function analyses indicate consistency with FN if the jumps in ν are not modelled in the arrival time analysis. Low-level activity is also evident between these events, but analysis of the residuals excluding the jumps produces inconclusive results due to low signal-to-noise ratios.

PSR 1323−58. The results for this pulsar are roughly consistent with FN (particularly the SF results). There are no significant events in ν or $\dot{\nu}$.

PSR 1323−62. The strength parameter and structure function results suggest consistency with FN. Two events in ν and one in $\dot{\nu}$ passed the threshold test.

PSR 1358−63. The results of the analyses show rough consistency with FN. One jump is resolved in both ν and $\dot{\nu}$.

PSR 1449−64. The results for this pulsar are inconclusive. There are no significant events in ν or $\dot{\nu}$. The data are well

described by a third-order polynomial. However, the derived amplitude of $\ddot{\nu}$ is too large to be due to pulsar spin-down, indicating that the observed activity may be due to an unresolved event in ν or $\dot{\nu}$.

PSR 1558−50. The timing noise of this pulsar is the largest in the whole sample. The results of the strength parameter analysis are inconsistent with a pure random walk process, whereas the structure function slopes show rough consistency with FN. Two events in $\dot{\nu}$ were found to be significant.

PSR 1641−45. This pulsar has undergone three period discontinuities (two large and one small) in the time interval 1977–1989 (Manchester et al. 1978, 1983; Flanagan 1993). Our observations span the most recent event (in 1989), and so the data were analysed in two ways, by using the phase residual data which (i) did not include the jump (modelled in the arrival time analysis), and (ii) included the jump. For method (i), the strength parameter results are not consistent with a pure random walk process, whereas the structure function slopes are roughly consistent with FN. For method (ii), the strength parameter results are similar to method (i), whereas the third-order structure function slope is much larger. In fact, the structure function results are roughly consistent with SN. This could be due to the jump in $\dot{\nu}$ identified by Flanagan. The fractional changes in ν and $\dot{\nu}$ derived from our data agree with those of Flanagan (1993) within the 2σ level. However, a threshold test on the jump indicates that only $\Delta\nu$ is significant. Another jump in ν is also significant.

PSR 1648−42. Large measurement uncertainties make it difficult to meaningfully probe the data for this pulsar. The present results are inconsistent with a pure random walk process, and the single event tested was not significant at the 5σ level.

PSR 1706−16. The results of the strength parameter analysis show rough consistency with FN, especially after third-order polynomial fits. This interpretation is supported by the structure function analysis, although the slope of $D^{(3)}_{\delta\phi}$ is larger than expected (close to 4). This can arise as a result of an event in $\dot{\nu}$. In fact, three events were found to be significant, two in ν and one in $\dot{\nu}$.

PSR 1737−30. This pulsar undergoes period discontinuities at a greater rate than any other known pulsar (McKenna & Lyne 1990). Analyses were carried out on phase residual data which both included and excluded four discrete jumps. The phase residual data excluding the jumps show a large cubic term, whose amplitude is much too large to be due to pulsar braking. It is possible that this third-order term is due to relaxation from previous glitches. The phase residual data including the jumps is shown in Fig. 1. A large jump (glitch) occurred at approximately TJD 9240, but it was not included in these analyses. This glitch was modelled in the arrival time analysis which produces the post-fit phase residuals. The strength parameter and structure function analyses gave results which are inconsistent with a pure random walk process, using both sets of data. Instead, most activity seems to be due to discrete events, although least-squares fits between events show that additional activity is present. All four events in ν are significant, but they do not appear to be accompanied by a significant jump in $\dot{\nu}$.

PSR 1737−39. Timing activity is not attributable to a pure random walk process or distinct events. The large third-order structure function slope (~ 4.0) indicates that some of the observed activity may be due to one or more unresolved events in $\dot{\nu}$. One such event is almost significant (Table 5).

PSR 1742−30. Strength parameters and structure function analyses give results which are not attributable to a pure random walk process or distinct events. The phase residuals after a third-order fit show little evidence of timing activity. However, the implied value of $\ddot{\nu}$ is too large to be due to pulsar spin-down. The structure function analysis gave a large slope for $D^{(3)}_{\delta\phi}(>6)$, indicating that most of the observed activity may be due to an unresolved event in $\dot{\nu}$.

PSR 1749−28. The results are not consistent with a pure random walk process. The significance tests demonstrate that discrete events produce much of the timing activity of this object. Three events are significant, one in ν and two in $\dot{\nu}$.

Five of the pulsars in our timing survey overlap with the JPL sample of objects studied by Cordes & Downs (1985), namely PSR 0628−28, 0736−40, 1706−16, 1749−28 and 2045−16. The data from our observations of PSR 2045−16 show little timing activity (see D'Alessandro et al. 1993), whereas the JPL data show a significant cubic term which Cordes & Downs have attributed to jumps in $\dot{\nu}$. It appears that there have not been any significant jumps during the 7-yr interval that we have been observing this pulsar. For PSR 0628−28, our results are roughly consistent with PN, and the level of timing activity over this time interval is less than that found by Cordes & Downs. These authors found that a pure random walk process was not responsible for the timing activity. Instead, one jump in $\dot{\nu}$ was found to be significant. Our data indicate that a jump in ν is statistically significant. However, the event in $\dot{\nu}$ found by Cordes & Downs can easily account for the difference in the level of timing noise. One interpretation of observed differences in the consistency (or lack thereof) with a random walk process is discussed below. The results for the remaining three pulsars are similar to those obtained from the JPL data, with the exception of PSR 1707−16. We have observed three microjumps, whereas none of the events tested in the JPL data set were significant.

As a final point, it is worthwhile considering the effect of the time span of the data on the results obtained from the analyses. It is possible that the slope of the power spectrum of the phase fluctuations in some pulsars steepens towards lower cyclical frequencies (longer time-scales), i.e., the fluctuations have a composite spectrum. Both Alpar et al. (1986) and Cheng (1987a,b) have discussed this possibility in relation to their theories of timing noise. In relation to the time domain analyses presented in this paper, a composite spectrum of phase fluctuations could show consistency with PN if the time span of the data probed is relatively short, FN over longer time spans, and SN over very long time spans.

Alternatively, a composite spectrum could be one explanation for results which do not show consistency with a pure random walk process. This is especially true if the power at a given cyclical frequency is underestimated because the observing time-scales ($t_{\rm obs}$) are smaller, or not much longer, than the time-scales of the variations due to timing noise ($t_{\rm TN}$). A similar problem has been discussed by Deshpande & Nityananda (1990) in connection with refractive scintillations. They have shown that the modulation amplitude of

long-term (refractive) intensity variations of pulsars can be substantially underestimated if the observing time spans are not much longer than the variations themselves.

4 CONCLUSIONS

Three different time domain analyses have been performed on the phase residuals of 45 pulsars. We find that (i) the present level of timing activity of 19 pulsars is too small to obtain meaningful results, (ii) the timing activity of seven pulsars is consistent with a pure random walk process (five with PN, two with FN), (iii) the timing activity of seven pulsars can be attributed to microjumps superimposed on a random walk process, (iv) the timing activity of seven pulsars can be attributed to microjumps plus other low-level activity, and (v) the timing activity of five pulsars is unidentified or unresolved. These results demonstrate that most timing activity is not solely due to a pure random walk in one of the rotation variables. The data for only seven out of the 26 pulsars analysed in detail show consistency with a pure random walk process.

The phase residuals of three pulsars in category (v) are well described by a large cubic term plus white noise. The cubic term could easily arise from a microjump in ν or $\dot{\nu}$, in which case these pulsars would be put into category (iv). The microjumps in ν and $\dot{\nu}$ observed from pulsars in categories (iii) and (iv) have amplitudes of both signs, with $|\Delta\nu| \simeq 5\times10^{-10}$–$2\times10^{-8}$ Hz and $|\Delta\dot{\nu}| \simeq (1\text{–}10)\times10^{-16}$ Hz s^{-1}.

Recent theories of physical mechanisms responsible for the observed timing noise have concentrated on torque variations both internal to the neutron star, and those originating from the pulsar magnetosphere (Cordes & Greenstein 1981; Alpar et al. 1986; Cheng 1987a,b; Cheng et al. 1988; Jones 1990).

Alpar et al. (1986) have proposed and discussed three models for timing noise. The range of 'event signatures' resulting from the present work, along with those found by Cordes & Downs (1985) and Cordes et al. (1988), show that none of these models, by themselves, predict the varied nature of the observed microjumps.

Cheng (1987b) has presented an extended model of timing noise in which (i) the high-frequency end of the timing noise power spectrum results from small-scale internal superfluid unpinning (microglitches), and (ii) the low-frequency end results from a sudden change of the current braking torque, which is perturbed by the microglitches. There is a degree of support for this model, since some of the observed timing activity cannot be attributed to a *pure* random walk process. Further investigation of this model necessitates the estimation of timing noise power spectra, which is beyond the scope of the present work. However, the model does not appear to address the fact that the bulk of the timing activity of a number of pulsars is due to a small number of discrete events in ν and $\dot{\nu}$, which can be of either sign.

Jones (1990) has proposed a theoretical model to explain the occurrence of microjumps in ν and $\dot{\nu}$ of either sign, as well as the observed 'two-component' power spectra of some pulsars. The model requires the existence of separate regions of pinned and corotating superfluid vortices within the neutron star, and appears to account for most of the results from analyses of timing noise.

Further comparisons of the observations and theories are necessary. By testing theoretical models such as these, observations of the timing activity of pulsars ultimately provide a further avenue to probe the structure and dynamics of neutron stars.

REFERENCES

Alpar M. A., Nandkumar R., Pines D., 1986, ApJ, 311, 197
Boynton P. E., Deeter J. E., 1986, preprint
Boynton P. E., Groth E. J., Hutchinson D. P., Nanos G. P., Partridge R. B., Wilkinson D. T., 1972, ApJ, 175, 217
Cheng K. S., 1987a, ApJ, 321, 799
Cheng K. S., 1987b, ApJ, 321, 805
Cheng K. S., Alpar M. A., Pines D., Shaham J., 1988, ApJ, 330, 835
Cordes J. M., 1980, ApJ, 237, 216
Cordes J. M., Downs G. S., 1985, ApJS, 59, 343
Cordes J. M., Helfand D. J., 1980, ApJ, 239, 640
Cordes J. M., Greenstein G., 1981, ApJ, 245, 1060
Cordes J. M., Downs G. S., Krause-Polstorff J., 1988, ApJ, 330, 847
D'Alessandro F., McCulloch P. M., King E. A., Hamilton P. A., McConnell D., 1993, MNRAS, 261, 883
Deeter J. E., 1984, ApJ, 281, 482
Deeter J. E., Boynton P. E., 1982, ApJ, 261, 337
Deshpande A. A., Nityananda R., 1990, A&A, 231, 199
Flanagan C. S., 1993, MNRAS, 260, 643
Groth E. J., 1975, ApJS, 29, 443
Jones P. B., 1990, MNRAS, 246, 364
Lindsey W. C., Chie C. M., 1976, Proc. IEEE, 64, 1652
Manchester R. N., Newton L. M., Goss W. M., Hamilton P. A., 1978, MNRAS, 184, 35P
Macnhester R. N., Newton L. M., Hamilton P. A., Goss W. M., 1983, MNRAS, 202, 269
McCulloch P. M., Klekociuk A. R., Hamilton P. A., Royle G. W. R., 1987, Aust. J. Phys., 40, 725
McCulloch P. M., Hamilton P. A., McConnell D., King E. A., 1990, Nat, 346, 822
McKenna J., Lyne A. G., 1990, Nat, 343, 439
Rutman J., 1978, Proc. IEEE, 66, 1048